Electronic Supplementary Information

Highly Efficient Flexible $MAPbI_3$ Solar Cells with Fullerene Derivative Modified SnO_2 Layer as the Electron Transport Layer

Meiyan Zhong, [a] Yongqi Liang,*[a] Jianqi Zhang, [b] Zhixiang Wei, [b] Qi Li, [a] and Dongsheng Xu, *[a]

[a] Beijing National Laboratory for Molecular Sciences, State Key Laboratory for Structural Chemistry of Unstable and Stable Species, College of Chemistry and Molecular Engineering, Peking University, Beijing 100871, PR China

[b] Key Laboratory of Nanosystem and Hierarchical Fabrication, National Center for Nanoscience and Technology, Beijing 100190, PR China.

yongqi.liang@pku.edu.cn

dsxu@pku.edu.cn

Experimental Section

Materials

Lead (II) iodide and SnO_2 colloid precursor (tin (IV) oxide, 15 wt % in H_2O colloidal dispersion) were purchased from Alfa Aesar. CPTA(C_{60} pyrrolidine tris-acid) was purchased from Sigma-Aldrich. MAI and Spiro-OMeTAD(2,2',7,7-tetrakis(N,Ndi-p-methoxyphenylamine)-9,9-spirobifluorene) were purchased from Xi'an Polymer Technology Co. (China). FK209 was bought from Dyesol Co. (Australia). Other chemicals were purchased from J&K Scientific, Ltd. (China) and they were used without further purification unless otherwise specified.

Device Fabrication

ITO/PEN (polyethylene naphthalate) substrates with a resistance <15 Ω/square were cleaned by isopropanol and then treated by O_2 plasma for 6 min. For SnO_2 fabrication, aqueous solution SnO_2 nanoparticles were diluted to the concentration of 2.5 wt % and then spin coated on the ITO/PEN substrate at 4000 rpm for 30 s followed by annealing at 140 °C for 30 min under ambient condition. Then 1mg/ml CPTA solution in DMF or 1mg/ml PCBM solution in chlorobenzene was spin coated at 2000 rpm for 30s followed by annealing at 80°C for 30 min in a N_2 filled glovebox. For $MAPbI_3$ precursor solution, 1.2 M of PbI_2 and MAI were dissolved in a mixture of DMF and DMSO (v/v, 7:3). Then the precursor solution was dropped on the substrate and spin coated at 3500 rpm for 30s with a chlorobenzene (CB) treatment 10 s after the spin-coating began. The prepared film was then heated on a hotplate at 100 °C for 35min. After cooling to room temperature, a 50 μL Spiro-OMeTAD solution was spin coated at 5000 rpm for 30 s. The spiro-OMeTAD solution was prepared by dissolving 73 mg Spiro-OMeTAD into 1 mL chlorobenzene followed by the addition of 29 μL 4-tert-butylpyridine, 18 μL Li-TFSI (520 mg/mL in acetonitrile) and 29 μL FK209 (300 mg/mL in acetonitrile). Finally 70 nm patterned Au was deposited by thermal evaporation as the top electrode.

Characterizations

The crystal structures of the perovskite films were measured by X-ray diffraction (Rigaku D/max-2500 diffractometer using Cu Kα radiation, λ =0.1542 nm), 8° $\min^{-1}$. The absorption spectra of the perovskite films were characterized by an UV/Vis spectrophotometer (Hitachi U-4100). Morphological images of perovskite films were observed by field emission scanning electron microscopy (Hitachi S-4800). AFM (Dimension Fastscan, Bruker, contact mode) was used to characterize the surface morphology. XPS measurements were carried out using a Kratos Axis Ultra system. The Raman characterization were carried out on DXRxi Raman Microscope (Thermo Fisher Scientific, USA) with an excitation wavelength of 532 nm. Steady-state PL were measured using a PL spectrometer (Edinburgh Instruments, FLS 920) with Xenon as the excitation source (excitation at 470 nm). TRPL spectra were measured at room temperature using a fluorescent spectrophotometer Delta flex. A Hamamatsu 479 nm diode laser was used as the excitation source.

Photocurrent density-voltage ($J – V$) curves were performed on a Keithley 2400 semiconductor characterization system under simulated AM 1.5 sunlight at 100 mW cm^{-2} irradiance produced by a Newport-69911solar simulator in the air. The scan rate was 0.1 V s^{-1}. During J-V measurements, a calibrated Si solar cell from Newport Corp. was used to calibrate the light intensity. For open-circuit photovoltage decay (OCVD) characterization, the perovskite device was directly connected to a digital oscilloscope (Lecroy, Wavesurfer 64Xs), and the sampling resistor was 1 MΩ to simulate the open-circuit condition. A pulse laser (532 nm, pulse width: 7 ns) was irradiated on the device to generate the photovoltage. The evolution of the photovoltage decay process after light excitation was recorded in the oscilloscope. The active area of the device is 0.1 cm^2, which is defined by a metal mask. According to the literature[1], the bending test of the flexible solar cells was carried out via a set of stainless steel rods with defined diameters. The perovskite solar cells on flexible substrates were brought into conformal contact to the rod, and remain for a short while (~3 seconds) during each cycle of bending (**Scheme. S1**).

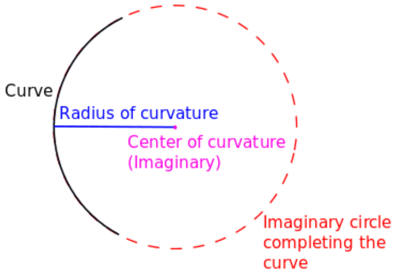

Scheme. S1 The terminology of curvature radius for bending test of flexible solar cells

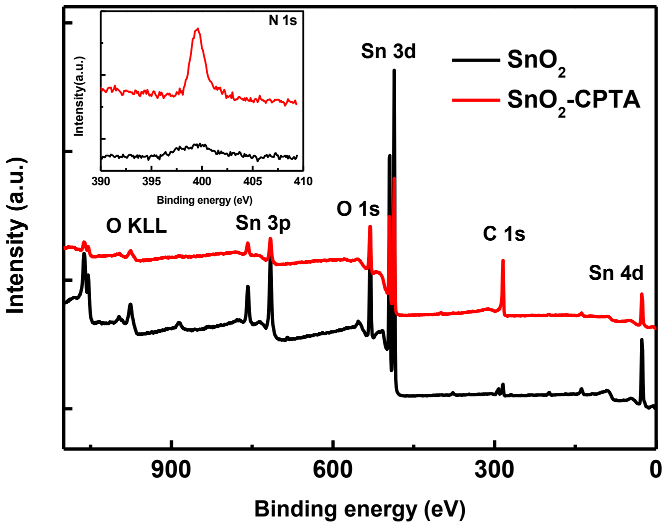

Fig. S1 XPS survey scans for CPTA modified SnO$_2$ and bare SnO$_2$. Inset: High-resolution XPS at N1s level. The presence of the N1s peak at 399.6eV and a much higher C1s peak at 284.5 eV proves the existence of the CPTA modifying layer.

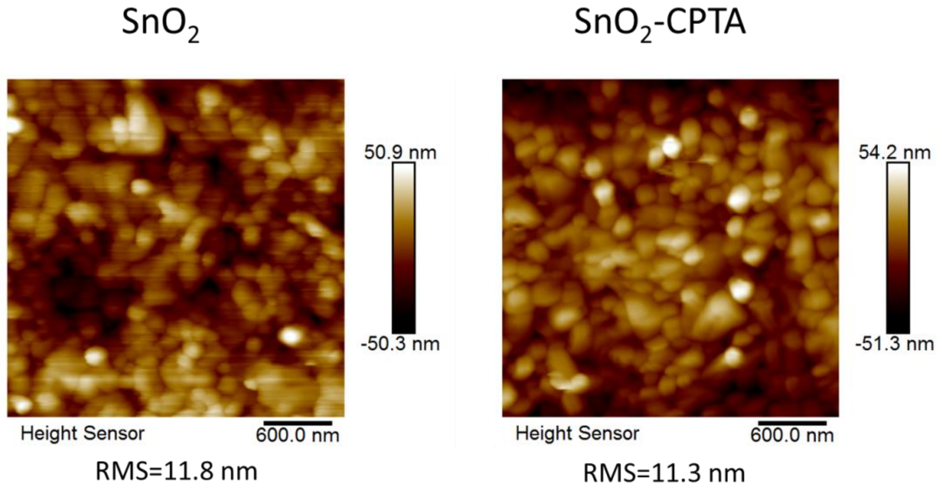

Fig. S2 Surface morphology of $CH_3NH_3PbI_3$ films grown on a) SnO_2 and b) SnO_2/CPTA substrate. The root-mean-square (RMS) roughness of the $MAPbI_3$ film on SnO_2-CPTA substrate is 11.3nm, and the RMS roughness of the $MAPbI_3$ film on SnO_2 substrate is 11.8nm.

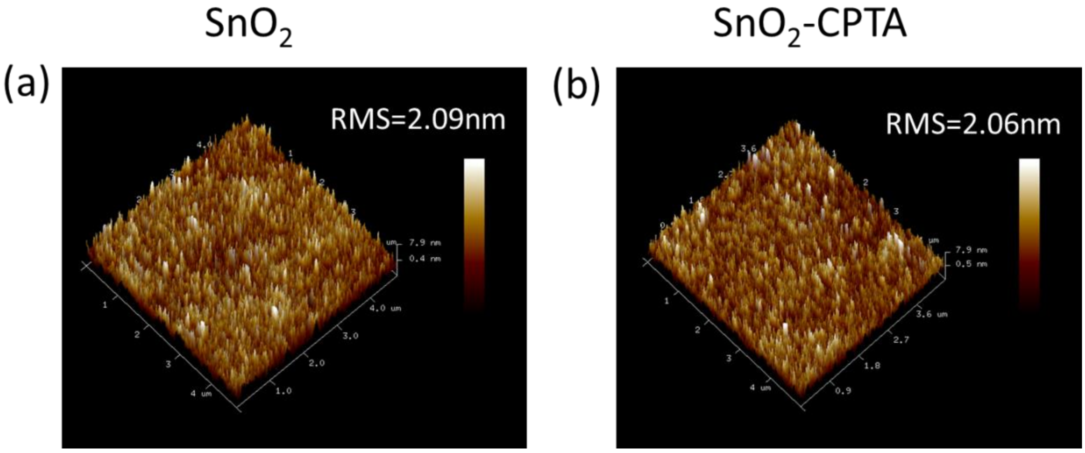

Fig. S3 AFM 3D views of (a) the SnO$_2$ film and (b) a CPTA film coated onto the SnO$_2$ substrate. The root-mean-square roughness (RMS) value (2.06 nm) of the CPTA-coated SnO$_2$ film was almost same as the RMS of 2.09 nm on the SnO$_2$ substrate without treatment. This indicates that the CPTA modification of the SnO$_2$/ITO substrates at least will not affect the MAPbI$_3$ films, from the view of roughness.

As shown in **Fig. S3**, the root-mean-square (RMS) roughness (2.06 nm) of CPTA-modified SnO$_2$ substrate is almost the same as that for the bare SnO$_2$ substrates. This indicates that the CPTA modification of the SnO$_2$ substrates will not affect the roughness of MAPbI$_3$ films (**Fig. S2**).

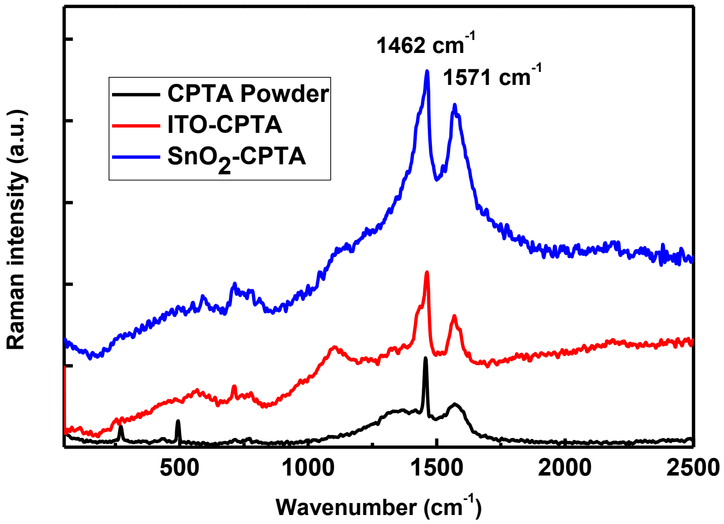

Fig. S4. Raman spectrum of CPTA powder, CPTA film based on ITO substrate and SnO$_2$-ITO substrate. The peaks at 1462 cm^{-1} and 1571 cm^{-1} can be assigned to the vibrations of C$_{60}$ rings[2], which indicate the presence of CPTA on the SnO$_2$ surface.

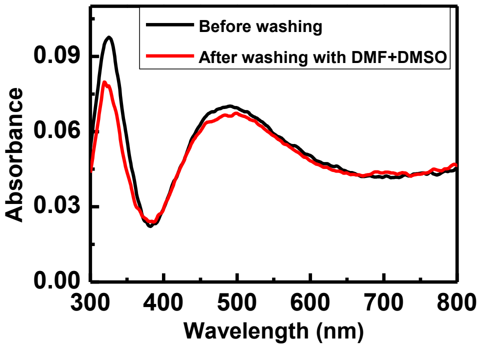

Figure. S5 Ultraviolet–visible (UV–Vis) absorbance spectra of CPTA (1mg/ml in DMF) on SnO_2-ITO substrate after washing with mixed solvent of DMF: DMSO (7:3, v/v).

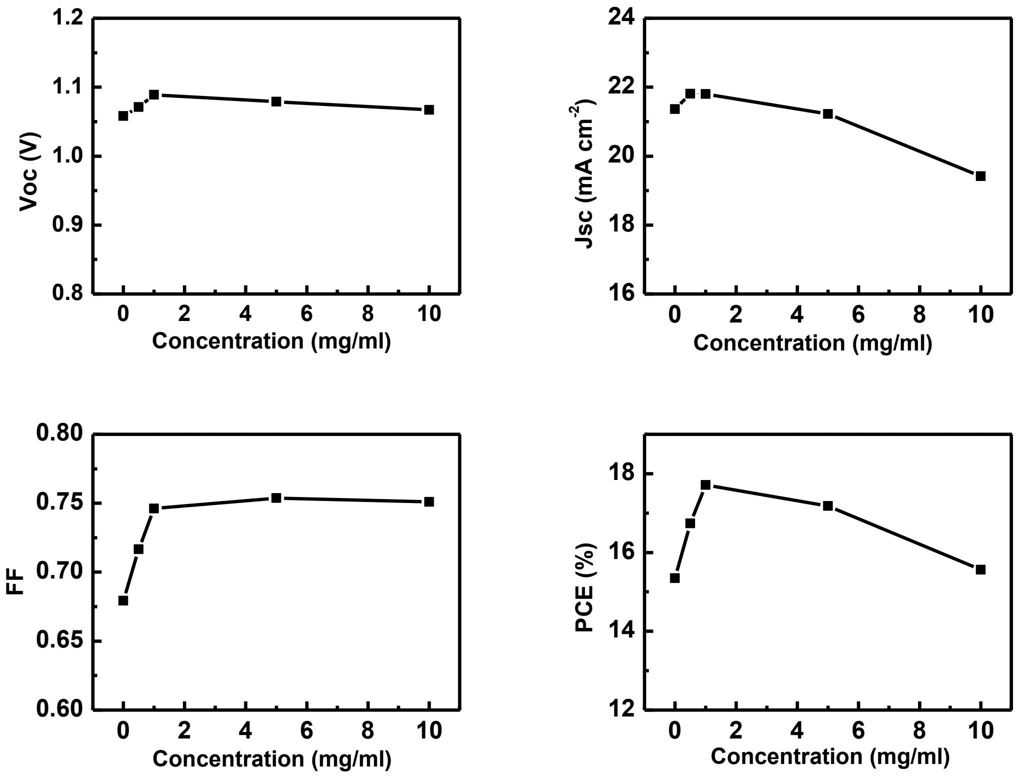

Fig. S6 Photovoltaic parameters (V_{OC}, J_{SC}, FF, PCE) as a function of the concentration of CPTA for a batch of $MAPbI_3$ solar cells. Note that the presence of CPTA layer has obvious effects on improving V_{OC} and FF. As the concentration of CPTA (DMF solution) increases from 0 to 10 mg/ml, the PCE firstly increases (up to 1 mg/ml) and then decreases. As a result, 1 mg/ml was selected during our following experiments.

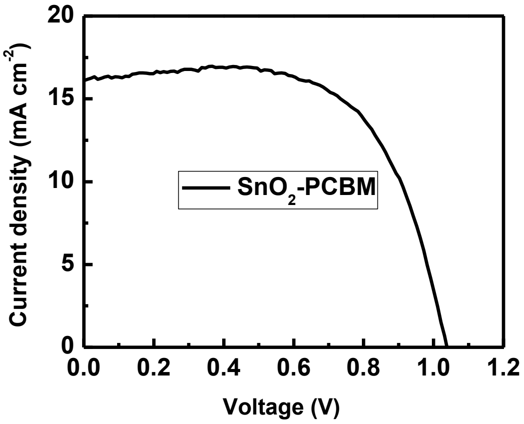

Fig. S7 J–V curve of the device based on SnO_2-PCBM electron transport layer.

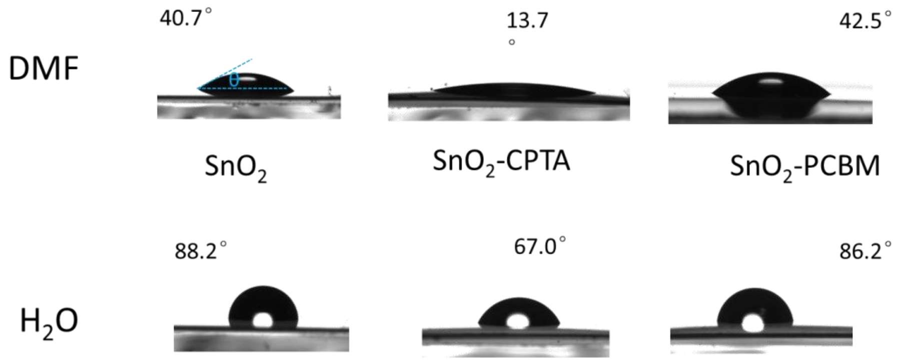

Fig. S8 Images of DMF and deionized water droplets demonstrating different contact angles on various surfaces without and with fullerene-derivative-coated on SnO_2 film.

The surface wetting behavior at the interface between the perovskite and CPTA is an important aspect of solution processing during perovskite crystallization. We conducted contact-angle measurements using N, N-dimethyl formamide (DMF) and deionized water (**Fig. S8**). These three substrates all exhibit poor water wetting properties whether or not the SnO_2 substrates are coated with fullerene derivatives, as confirmed by the large contact angles of water. Moreover, For DMF droplets, SnO_2/CPTA shows a lower contact angle than pure SnO_2 and SnO_2/$PC_{61}BM$, indicating that the carboxyl groups from CPTA molecules could improve the wettability effectively.

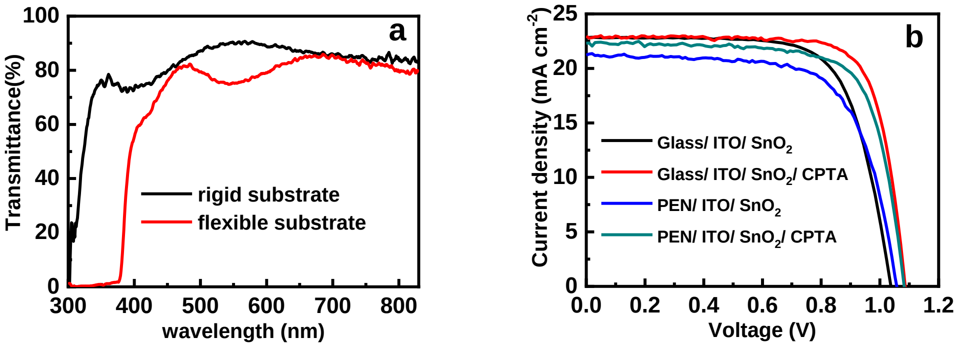

Fig. S9 (a) Transmittance spectra of ITO/glass and ITO/PEN substrates; (b) J-V curves of PSCs with different ETLs based on rigid and flexible substrates. The flexible conductive substrates show lower transmittance in the visible range due to the lower transparency of the polymer substrate.

The transmittance spectra of ITO/glass, ITO/PEN substrates are shown in **Fig. S9**. For flexible and rigid devices, modification of SnO_2 with CPTA improve the power conversion efficiencies obviously. The flexible conductive substrates show lower transmittance in the visible range due to the lower transparency of the polymer substrate, which in turn causes poor current density and PCE of those devices.

Table S1. Photovoltaic performance metrics obtained from $MAPbI_3$-based perovskite solar cells with various substrates (under AM 1.5G illumination at 100 mW cm^{-2}).

Substrates	**V_{OC} (V)**	**Jsc (mA cm^{-2})**	**FF**	**PCE (%)**
PEN/ITO/SnO_2	1.058	21.36	0.68	15.35
PEN/ITO/SnO_2/PCBM	1.039	16.19	0.66	11.13
PEN/ITO/SnO_2/CPTA	1.083	22.39	0.75	18.36
Glass/ITO/SnO_2/CPTA	1.086	22.78	0.77	19.14
Glass/ITO/SnO_2	1.039	22.83	0.71	16.91

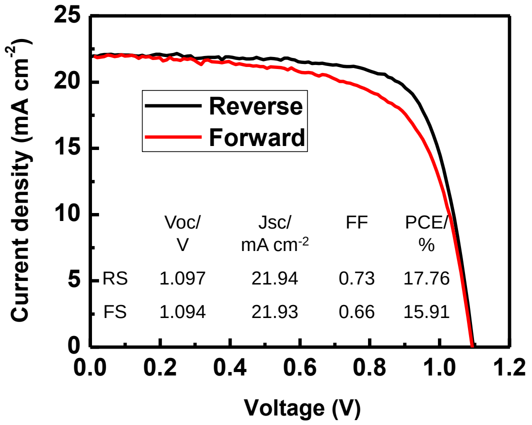

	Voc/ V	Jsc/ mA cm^{-2}	FF	PCE/ %
RS	1.097	21.94	0.73	17.76
FS	1.094	21.93	0.66	15.91

Fig. S10 J–V curves of flexible MAPbI$_3$ Solar Cells under both reverse and forward scan directions based on SnO$_2$-CPTA substrate. From forward bias to short circuit condition (reverse scan direction, black), from short circuit to forward bias condition (forward scan, red)

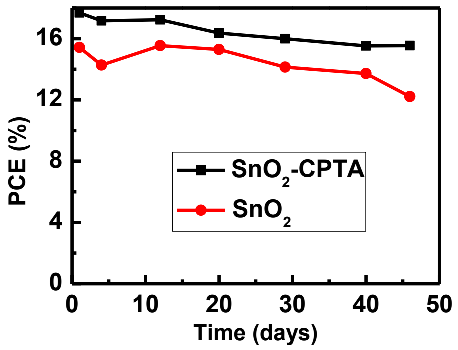

Fig. S11 The stability measurements of flexible devices deposited on different ETL without any encapsulation exposed at atmospheric environment of ≈30% humidity in the dark. The measured efficiency of SnO$_2$/CPTA based devices remained at 87% of the initial optimized value 46 d under ambient environment (25°C, 30% relative humidity level) without encapsulation, while SnO$_2$ based devices remained 80%.

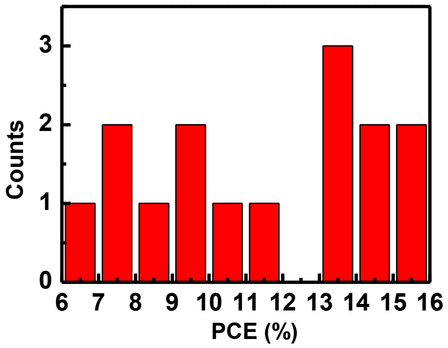

Fig. S12 Histogram of the power conversion efficiency for 15 flexible $MAPbI_3$ devices with SnO_2 ETLs. We only fabricated 15 devices to confirm the reproducibility of PSCs based on SnO_2 substrate without treatment and the average PCEs were 11.52 ±3.1%. Thus, adding CPTA to SnO_2 substrate can improve devices reproducibility.

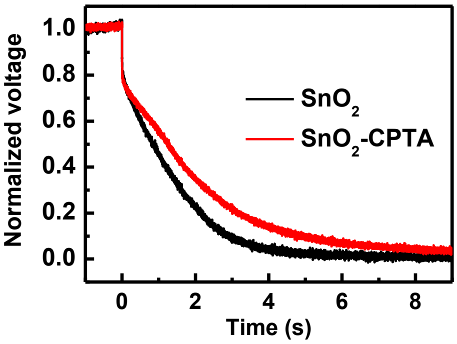

Fig. S13 Open-circuit photovoltage decay (OCVD) curves of solar cells based on bare-SnO_2 and CPTA modified SnO_2 electron transport layer.

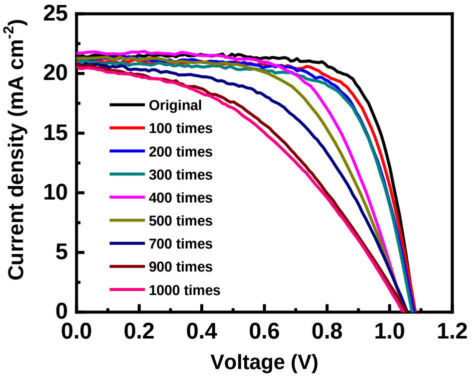

Fig. S14 *J*-*V* curves of a flexible perovskite solar cell measured under reverse scans after various bending cycles.

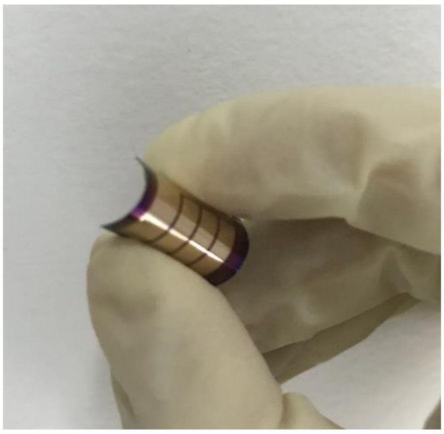

Fig. S15 Photograph of a flexible $MAPbI_3$ solar cell deposited on PEN substrate with the SnO_2-CPTA Electron transport layer.

Table S2. Summarized Emission Lifetime and Corresponding Intensities for Various Perovskite Samples Obtained Using Two Exponential Decay Model.

Samples	**B1 (%)**	**τ1 (ns)**	**B2 (%)**	**τ2 (ns)**	**Average τ (ns)**[3]
PEN/ITO/SnO_2	58.4	69.73	41.6	266.35	214
PEN/ITO/SnO_2-PCBM	19.2	23.14	80.8	171.90	167
PEN/ITO/SnO_2-CPTA	45.2	12.32	54.8	116.68	108

1. J. Yoon, H. Sung, G. Lee, W. Cho, N. Ahn, H. S. Jung and M. Choi, *Energy Environ. Sci.*, 2017, **10**, 337-345.
2. K. L. Akers, C. Douketis, T. L. Haslett, M. Moskovits, *J. Phys. Chem*. 1994, **98**, 10824-10831.
3. D. Yang, R. Yang, J. Zhang, Z. Yang, S. Liu, C. Li, *Energy Environ. Sci*. 2015***, 8***, 3208-3214.